Growth and Structure of Fullerene Thin Films and Other Carbon Nanomaterials

E.A. Katz[*], O. Prilutskiy[**], D. Faiman[*], S. Shtutina[***], V. Ezersky[****] and E. Mogilko[*****]

[*]Department of Solar Energy and Environmental Physics, J. Blaustein Institute for Desert Research, Ben-Gurion University of the Negev, Sede Boqer, 84990 Israel,
[**]CMC Ltd., POB 633, Ofakim 80300 Israel
[***]Department of Physics, Ben-Gurion University of the Negev, Beersheba, 84105 Israel
[****] Department of Materials, Ben-Gurion University of the Negev, Beersheba, 84105 Israel
[*****]Department of Physics and Center for Superconductivity, Bar-Ilan University, Ramat Gan, 52900 Israel

ABSTRACT

The present paper reports relationships between structural characteristics of carbon materials and conditions of their production.

C_{60} thin films were grown by a vacuum deposition technique on various substrates. We demonstrate effect of the substrate material and temperature as well as the deposition rate on the crystalline structure of the films, as measured by X-Ray Diffractometry (XRD) and Atomic Force Microscopy (AFM).

Multiwalled carbon nanotubes (MWCNTs) and various nanoclusters, such as carbon-encapsulated nanoclusters of Fe and Fe_3O_4, were produced by a catalytic disproportionation of carbon monoxide. Structure of these nanomaterials was studied by Transmission Electron Microscopy (TEM) and High Resolution Transmission Electron Microscopy (HRTEM), Energy Dispersive Spectrum (EDS) analysis and XRD.

Keywords: fullerene thin films, carbon nanotubes, nanocapsules.

1. EXPERIMENTAL DETAILS

C_{60} thin films were grown by a vacuum deposition technique on substrates of optical glass, mica and optical glass predeposited with an Ag sub-layer. The starting C_{60} powder ('Super Gold Grade', > 99.9% purity) was commercially obtained from Hoechst AG. The vacuum chamber pressure was maintained at about 8×10^{-7} Torr. A detailed description of the deposition conditions has been given elsewhere [1-4].

The thickness of the C_{60} films was about 100 nm.

The crystalline structure of the C_{60} thin films was first characterized by powder XRD in Cu-K_α at room temperature, and then by temperature-resolved XRD over the temperature range 15 - 300 K [5].

Morphology of the front surface of the C_{60} films was studied by Atomic Force Microscopy (AFM).

Carbon nanotubes and nanocapsules were produced by a catalytic disproportionation of carbon monoxide.

A Fe_2O_3 powder of a specific surface area of 15 m^2/g was placed in a Cu crucible and heated up to 540 – 600 °C in CO gas flowing through a quartz tube reactor at a rate of 0.5 l/min.

Products of the reaction, collected from the crucible and the reactor, were studied by TEM, HRTEM, EDS and XRD.

2. RESULTS AND DISCUSSION

2. 1. C_{60} thin films

Our approach for the deposition of well-ordered C_{60} films requires a combination of high deposition rates and high substrate temperatures (close to the temperature of the "adsorption (deposition) ↔ desorption" equilibrium for C_{60} molecules), as well as utilization of a substrate with weak surface bonding to C_{60} [1, 3].

By varying the deposition conditions (material and temperature of substrate, evaporation and deposition rates), we grew films of three types differing widely in the morphology and crystalline structure.

Films of one type, represented by sample 1, were deposited at a rate of 0.2-0.4 Å/s on a glass substrate held at 170 °C. These growth conditions did not satisfy the above-mentioned requirements, thus resulting in a lower degree of crystallinity. Indeed, Sample 1 was found to consist of two phases: X-ray amorphous and polycrystalline with grain sizes of 20 - 50 nm. The latter was characterized by the Bragg reflections (111), (220) and (311) of *fcc* C_{60} lattice. The room-temperature XRD pattern of such a film is similar to one displayed in Fig. 2c in Ref. 2.

Films of the other type, represented by sample 2, deposited at a rate of 18-20 Å/s onto the Ag/glass substrate at 200 °C, were found to have high degree of crystallinity and strong <111>-texture. The room-temperature XRD pattern of this sample (Fig. 1) consists only of a very narrow and intensive (111) peak and its higher harmonics (222) and (333). The sizes of crystalline domains for sample 2 are relatively large. AFM measurements revealed grain sizes in the sample surface of about 200 nm.

A mica substrate also satisfies the above-mentioned requirement of weak surface bonding because it is a layered material with weak van der Waals interaction between layers. We succeeded in growing C_{60} thin films on a mica

substrate, with crystalline structure even better than that for the films deposited on a metal sub-layer. Films of this type are represented by sample 3. Sample 3 deposited at a rate of 15 Å/s onto a mica substrate, held at 200 °C also had strong <111>-texture. However, the intensities of the peaks in its room-temperature XRD pattern (not shown) were found to be substantially higher than those we observed for sample 2. The sizes of crystalline domains are also much larger. AFM revealed grain sizes in the sample surface of 500-1500 nm (Fig. 2).

Analysis of the XRD patterns for all polycrystalline C_{60} films studied points to the fact that the material at room temperature has *fcc* structure. Our room-temperature value of the lattice parameter a = 14.144 Å is in good agreement with the data published for C_{60} single crystals and powder bulk samples [6-8].

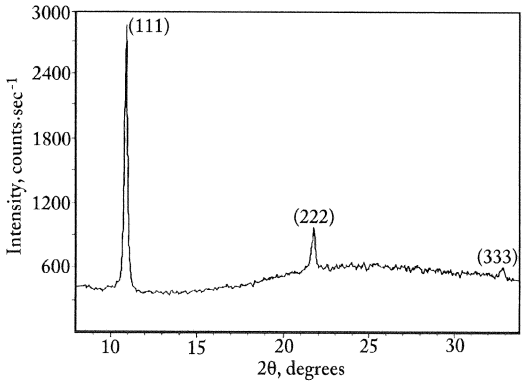

Fig. 1. Room temperature XRD pattern of sample 2

Temperature-resolved XRD study of our films [5] confirmed, in general, the accepted concepts concerning structural transformations that occur during the cooling of solid C_{60} and associated with changes in the molecular rotations. In particular, near the temperature T_c = 260 K C_{60} single crystals and powder bulk samples undergo a first order phase transition from *fcc* structure above T_c to *sc* structure below T_c [6]. C_{60} molecules have been shown to rotate freely in the *fcc* phase and the rotation locks into specific orientations in the *sc* phase. This disorder/order transition is accompanied by a discontinuity in lattice parameter $\Delta a/a \cong 0.31$ - 0.33 % [6-8]. Our textured films (samples 2 and 3) also undergoes a first order phase transition, i. e. a well defined discontinuity in the lattice parameter (see Table 1 and Ref. 5). This fact, in addition to the results of room temperature XRD, AFM and STM, points to the high quality of our films.

It should be noted, however, that the observed values of $\Delta a/a$ and T_c for our thin films are lower than those published for C_{60} bulk samples. Furthermore, we have demonstrated a reduction in the $\Delta a/a$ and T_c values with decrease of grain sizes in the C_{60} films (table I). This may be due to a relatively high density of crystalline defects (including grain boundaries), strains and impurities in C_{60} thin films, in comparison with single crystals.

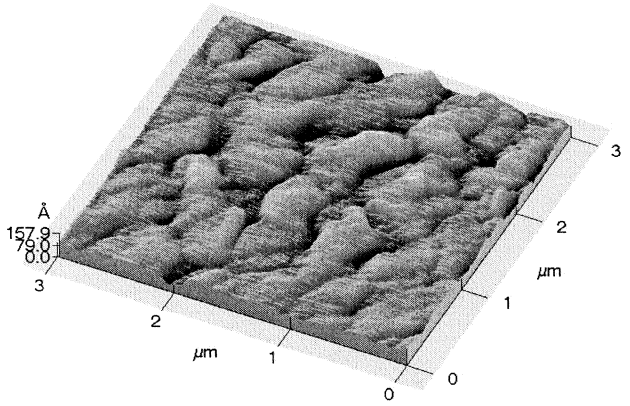

Fig. 2. AFM image of sample 3.

Sample	Crystalline structure of C_{60} films	Grain size in the film surface (nm)	T_c (K)	$\Delta a/a$ (%)
1	amorphous/ polycrystalline	20-50	-	-
2	<111> textured polycrystalline	200	250	0.06
3	<111> textured polycrystalline	500-1500	252	0.22
SC	-	-	260	0.31-0.33

Table I. Structural characteristics and parameters of the *fcc*/*sc* phase transition for our C_{60} thin films together with the published data [6-8] for C_{60} single crystals (SC).

2.2. Carbon nanotubes and nanocapsules.

Two main types of carbon nanoparticles, namely carbon nanotubes and nanocapsules, have been observed.

Diameter and length of the nanotubes were of 10 - 70 nm and 0.5 - 100 μm, respectively. HRTEM images of two nanotubes are shown in Figure 3. Many structural defects can be clearly seen. Among them, there are regions where graphite layers are not along the axis of the nanotube. These regions may be considered as parts of Multi-Walled Carbon Nano-Fibers (MWCNFs). The latter are characterized by non-zero angle between the graphite basal planes and the central axis while this angle is equal to zero in MWCNTs [9]. It is important to note that MWCNF are, in general, well aligned and useful as electrodes and field emitters as reported in Refs. 10 – 12.

According to literature data most of the carbon nanotubes, produced by various catalytic methods, are decorated by spherical carbon nanocapsules of a diameter of 5 – 100 nm, with a catalyst metal core [13]. In this paper, we suggest a new concept of production of such nanocapsules at the reactor sites spatially separated from the sites of deposition of other products of the process (carbon nanotubes, large carbon onions, amorphous carbon).

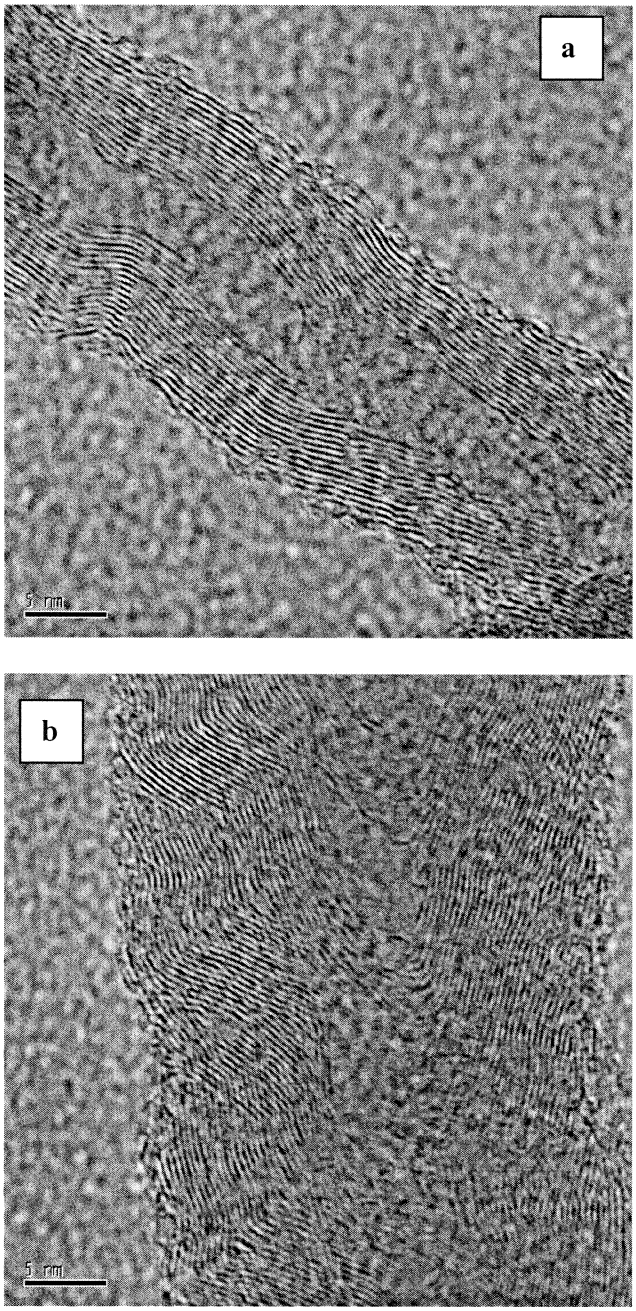

Fig. 3. HRTEM images of MWCNT.

Figure 4 shows HRTEM image of two carbon-encapsulated nanoclusters with defect-free crystalline structure. HRTEM micro-diffraction pattern, EDS analysis and XRD revealed that the nanocapsule cores consist of highly crystalline Fe_3O_4. Deposition of such nanoparticles, with a diameter of 2 –10 nm, has been found to occur at cooled parts of the reactor.

Figure 4 shows HRTEM image of two carbon-encapsulated nanoclusters with defect-free crystalline structure. HRTEM micro-diffraction pattern, EDS analysis and XRD revealed that the nanocapsule cores consist of highly crystalline Fe_3O_4. Deposition of such nanoparticles, with a diameter of 2 –10 nm, has been found to occur at cooled parts of the reactor.

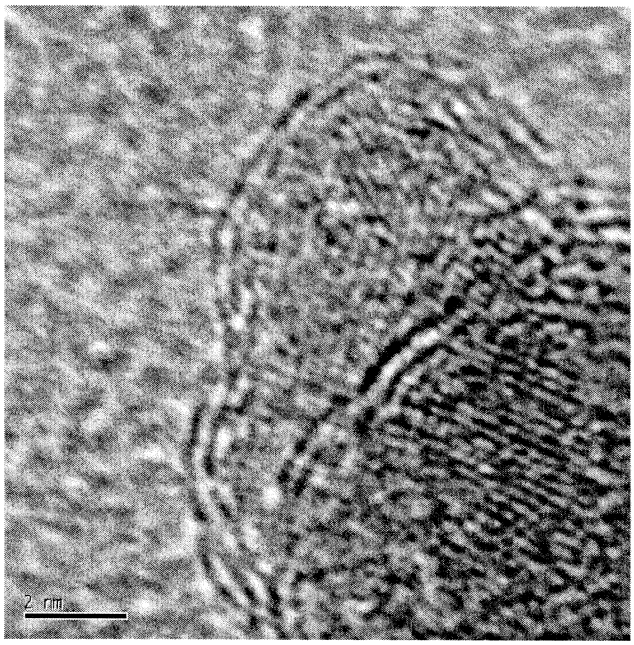

Fig. 4. HRTEM image of two carbon-encapsulated nanoclusters of Fe_3O_4.

We believe that the core-clusters are generated in the active zone of the reaction of carbon monoxide disproportionation, while carbon shells, encapsulating a core, are formed during a diffusion of the latter from the active zone of the reaction, in CO atmosphere. Indeed, movement of aerosol particles is known to be governed by diffusion rather than the gravitation and aerodynamic principles. In our experiment, the aerosol Fe_3O_4 particles have been found to diffuse along the temperature and concentration gradient from the active zone of the reaction in the directions along and even against (!) the gas flow. During their diffusion in CO atmosphere, these core nanoclustes also act as catalysts and instigate the formation of encapsulating carbon hells.

The encapsulating shells of the nano-clusters are stable in air at room temperature, but do not prevent them at elevated temperatures. Accordingly, these nanoparticles may act as catalysts for the corresponding production of carbon nanomaterials via carbon monoxide disproportionation. As a result of such a process, we have demonstrated, for example, a transformation from the Fe_3O_4 core to a nanoparticle of a pure Fe with a simultaneous formation of additional carbon encapsulating layers.

Figure 5 displays an HRTEM image of such a nanocapsule. One can clearly seen an ~ 10 nm Fe cluster encapsulated by as many as 6 concentric quasi-spherical carbon shells. The distance between the carbon layers are found to be close to that of graphite, 0.34 nm.

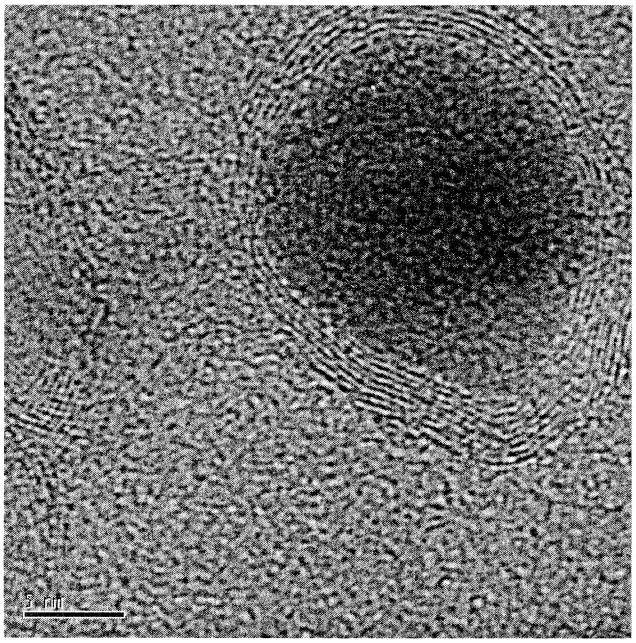

Fig. 5. HRTEM image of a carbon nanocapsule with a Fe core.

REFERENCES

1. 1. E.A. Katz, US Patent No: 5,876,790 (1999).
2. D. Faiman, S. Goren, E. Katz, M. Koltun, N. Melnik, A. Shames, and S. Shtutina, *Thin Solid Films* 295, 283 (1997).
3. E.A. Katz, D. Faiman, S. Shtutina, and A. Isakina, *Thin Solid Films* 368, 49(2000).
4. E.A. Katz, D. Faiman, S. Shtutina, A. Isakina, K. Yagotintsev, and K. Iakoubovskii, *Solid State Phenomena* 80-81, 15 (2001).
5. E.A. Katz, D. Faiman, S. Shtutina, A. Isakina, and K. A. Yagotintsev. In: *Nanotubes, Fullerenes, Nanostructed and Disordered Carbon*, Materials Research Society Symposium Proc., v. 675, 2001, ed. by J. Robertson, T.A. Friedmann, D.B. Geohegan, D.E. Luzzi, and R.S. Ruoff, p. W7.6.1.
6. P.A. Heiney, J.E. Fisher, A.R. McGhhie, W.J. Romanow, A.M. Denestejn, J.P. McCauley Jr., A.B. Smith III and D.E. Cox, *Phys. Rev. Lett.* 66, 2911 (1991).
7. H. Kasatani, H. Terauchi, Y. Hamanaka and S. Nakashima, *Phys. Rev. B* 47, 4022 (1993).
8. S. Fomenko, V. D. Natsik, S. V. Lubenets V. G. Lirtsman, N. A. Aksenova, A. P. Isakina, A. P. Prokhvatilov, M. A. Strzhemechny and R. S. Ruoff, *Low Temp. Phys.* 21, 364 (1995).
9. D. Nolan, D. C. Lynch and A. H. Cutler, *J. Phys. Chem. B* 102, 4165 (1998).
10. Z. F. Ren, Z. P. Huang, J. W. Xu, J. H. Wang, P. Bush M. P. Siegel and P. N. Provencio, *Science* 282, 1105 (1998).
11. Y. C. Choi, Y. M. Shin, S. C. Lim, D. J. Bae, Y. H. Lee, B. S. Lee and D. Chung, *J. Appl. Phys.* 88, 4898 (2000).
12. V. I. Merkulov, D. H. Lowndes, Y. Y. Wei, G. Eres and E. Voelkl, *Appl. Phys.Lett.* 76, 3555 (2000).
13. "Carbon Nanotubes: Synthesis, Structure, Properties and Applications", M. Dresselhaus, G. Dresselhaus and Ph. Avouris, Eds., Springer-Verlag, Berlin, 2001.